CrystEngComm

PAPER

View Article Online
View Journal | View Issue

Cite this: *CrystEngComm*, 2015, **17**, 4992

Nickel(II) and copper(I,II)-based metal-organic frameworks incorporating an extended tris-pyrazolate linker†

Aurel Tăbăcaru,[ab] Simona Galli,[c] Claudio Pettinari,[a] Norberto Masciocchi,[c] Thomas M. McDonald[d] and Jeffrey R. Long*[de]

Received 19th March 2015,
Accepted 19th May 2015

DOI: 10.1039/c5ce00561b

www.rsc.org/crystengcomm

Solvothermal reactions between the tritopic pyrazole-based ligand 1,3,5-tris((1*H*-pyrazol-4-yl)phenyl)benzene (H_3BTPP) and nickel(II) perchlorate or copper(II) nitrate afforded two new metal-organic frameworks, $Ni_3(BTPP)_2$·solvent (**Ni-BTPP**) and $Cu^{I}_4Cu^{II}_2(OH)_2(BTPP)_2$·solvent (**Cu-BTPP**). Powder diffraction structure determination methods were employed to determine the crystal and molecular structure of the copper(I,II) derivative: triangular [$Cu_3N_6(\mu_3$-OH)] nodes are connected to six nearby ones by the pyrazolate ligands, thus constructing flat two-dimensional layers that stack to form slit-like one-dimensional channels. Thermogravimetric analyses highlighted both the thermal stability and the permanent porosity of these two materials. Porosity was confirmed by N_2 adsorption at 77 K, yielding Langmuir specific surface areas of 1923(3) $m^2\ g^{-1}$ and 874(8) $m^2\ g^{-1}$ for **Ni-BTPP** and **Cu-BTPP**, respectively. Additionally, **Ni-BTPP** adsorbed 1.73 mmol g^{-1} (7.6 wt%) of CO_2 at the mild conditions of 298 K and 1 bar.

Introduction

Owing to the potential of metal-organic frameworks[1] (MOFs) for use in a broad range of applications, including luminescence,[2] magnetism,[3] adsorption,[4] catalysis,[5] separation,[4d–6] drug delivery and imaging,[7] the number of reported framework structures continues to increase rapidly. MOFs may offer substantial advantages with respect to the prototypical classes of porous inorganics (zeolites and activated carbons) in terms of versatility of the architectural topologies and the tunability of pore geometry and functionality.[8]

Poly(azolate) ligands have exhibited interesting coordination chemistry toward late transition metal ions, concurring to build up polymeric architectures featuring, *e.g.*, adsorptive, optical, catalytic or magnetic properties.[9] Examples of porous MOFs containing poly(azolate) bridging ligands include materials based upon bis- and tris(pyrazolates),[10] bis- and tris(triazolates),[11] and bis- and tris(tetrazolates).[12] Of particular interest are the sodalite-type MOFs constructed with 1,3,5-tris(1*H*-pyrazol-4-yl)benzene (H_3BTP),[10d] 1,3,5-tris(1*H*-1,2,3-triazol-5-yl)benzene (H_3BTTri),[11e] 1,3,5-tris(tetrazol-5-yl)benzene (H_3BTT)[12d] and 1,3,5-tri-*p*-(tetrazol-5-yl)phenylbenzene (H_3TPB-3tz),[12e] possessing exposed metal sites potentially suitable for the enhancement of CO_2 and H_2 adsorption.

Over the past few years, we have focused our attention on isolating and characterizing new poly(pyrazolate)-based MOFs. Due to the higher pK_a of pyrazole compared to triazole

[a] *Scuola di Scienze del Farmaco e dei Prodotti della Salute, Università di Camerino, Via S. Agostino 1, 62032 Camerino, Italy*
[b] *Department of Chemistry, Physics and Environment, Faculty of Sciences and Environment, "Dunarea de Jos" University of Galati, 111 Domneasca Street, 800201 Galati, Romania*
[c] *Dipartimento di Scienza e Alta Tecnologia, Università dell'Insubria, Via Valleggio 9, 22100 Como, Italy*
[d] *Department of Chemistry, University of California, Berkeley, California 94720, USA. E-mail: jrlong@berkeley.edu*
[e] *Materials Science Division, Lawrence Berkeley National Laboratory, Berkeley, California 94720, USA*

† Electronic supplementary information (ESI) available: Details on the synthesis of H_3BTPP. IR spectra for **Ni-BTPP** and **Cu-BTPP**. XRPD traces for **Ni-BTPP** and **Cu-BTPP**. Graphical result of the final Rietveld refinement for **Cu-BTPP**. BET fitting parameters of the N_2 adsorption isotherms for **Ni-BTPP** and **Cu-BTPP**. See DOI: 10.1039/c5ce00561b

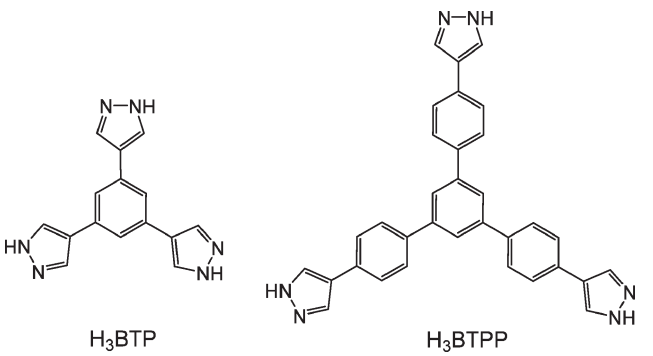

Scheme 1 Chemical structures of 1,3,5-tris(1*H*-pyrazol-4-yl)benzene (H_3BTP, left) and 1,3,5-tris((1*H*-pyrazol-4-yl)phenylene)benzene (H_3BTPP, right).

and tetrazole,[13] pyrazolate ligands generally provide stronger metal-to-ligand coordinative bonds, conferring extreme thermal and chemical robustness to the corresponding MOFs.[10a] Representative examples in this respect are the two $M_3(BTP)_2$ materials isolated by coupling H_3BTP (Scheme 1) to nickel(II) and copper(II):[10d] these two MOFs exhibit an expanded sodalite-like structure and feature metal sites that can be desolvated, hence exposed, without loss of porosity. Moreover, $Ni_3(BTP)_2$ is stable to heating in air to 430 °C, as well as to treatment with boiling aqueous solutions of pH 2 to 14 for two weeks.

Seeking to isolate pore-expanded homologs of the previously reported $M_3(BTP)_2$ materials, we synthesized for the first time 1,3,5-tris((1*H*-pyrazol-4-yl)phenyl)benzene (H_3BTPP, Scheme 1) for use as a potential linker. Here, we report the isolation of H_3BTPP and of two new MOFs, containing nickel(II) and copper(I,II), derived therefrom. The structural features of the copper(I,II) derivative are described, and the thermal stability and the adsorption performances of the two MOFs toward N_2 at 77 K and CO_2 at 298 K are discussed.

Experimental section

Materials and methods

All chemicals were purchased from Sigma Aldrich Co. and used as received without further purification. All solvents were used as received in their anhydrous form. ^{1}H-NMR spectra were recorded at 298 K on a Bruker Avance 400 instrument (400 MHz) in the NMR Facility of the University of California, Berkeley. Elemental analyses (C, H, N) were obtained from the Microanalytical Laboratory of the University of California, Berkeley. Infrared spectra were recorded in the range 4000–650 cm^{-1} on a Perkin Elmer Spectrum 100 Optica FTIR spectrometer. Thermogravimetric analyses were carried out at a ramp rate of 7 °C min^{-1} under a flow of nitrogen with a TA Instruments TGA Q5000. The magnetic susceptibilities were measured at room temperature (295 K) by the Gouy method, using a Sherwood Scientific Magnetic Balance MSB-Auto, using $HgCo(NCS)_4$ as calibrant and correcting for diamagnetism with the appropriate Pascal constants. The magnetic moments (in BM) were calculated from the equation $\mu_{eff} = 2.84(X_m^{corr}T)^{1/2}$. Preliminary chemical stability tests were carried out by suspending 10 mg samples of **Ni-BTPP** and **Cu-BTPP** in water at room temperature. The integrity of the recovered material was checked by PXRD.

1,3,5-Tris((1*H*-pyrazol-4-yl)phenyl)benzene (H_3BTPP)

As depicted in Scheme S1 of the ESI,† 1,3,5-tris((1*H*-pyrazol-4-yl)phenyl)benzene was synthesized by the Suzuki coupling reaction of 1,3,5-tris(4-bromophenyl)benzene and 1-(tetrahydro-pyran-2-yl)-4-pyrazoleboronic acid pinacol ester, following a slightly modified procedure with respect to the one reported in the literature.[14] Details on the synthetic procedure adopted and on the characterization of the ligand are available in the ESI.†

$Ni_3(BTPP)_2{\cdot}7DMF{\cdot}10H_2O$ (Ni-BTPP)

In a 100 mL glass jar, H_3BTPP (0.125 g, 0.247 mmol) and $Ni(ClO_4)_2{\cdot}6H_2O$ (0.543 g, 1.48 mmol) were dissolved in 75 mL of DMF : MeOH (2 : 1, v/v) under sonication for 5 min. **CAUTION**: perchlorates are potential explosives. The light green solution was subsequently heated at 100 °C for two days until an orange solid was formed. The precipitate was filtered off, washed twice with 20 mL of hot DMF and dried in air. Yield: 86%. **Ni-BTPP** is insoluble in alcohols, chlorinated solvents, acetonitrile, DMSO, DMF, acetone and H_2O. Elem. Anal. calc. for $C_{87}H_{111}Ni_3N_{19}O_{17}$ (FW = 1871.02 g mol^{-1}): C, 55.85; H, 5.98; N, 14.22%. Found: C, 55.75; H, 5.65; N, 14.37%. IR (neat, cm^{-1}): 3375(br), 3025(vw) ν(C–$H_{aromatic}$), 2918(w) ν(C–$H_{aliphatic}$), 1654(vs) ν(C═O), 1560(m), 1498(w) ν(C═C + C═N), 1384(s), 1252(m), 1092(s), 1057(m), 956(s), 821(vs), 659(s).

$Cu^I_2Cu^{II}(OH)(BTPP){\cdot}3DMF{\cdot}H_2O$ (Cu-BTPP)

In a 100 mL glass jar, H_3BTPP (0.125 g, 0.247 mmol) and $Cu(NO_3)_2{\cdot}2.5H_2O$ (0.344 g, 1.482 mmol) were dissolved in 70 mL of DMF : MeOH (1 : 1, v/v) under sonication for 5 min. The light blue solution was heated at 80 °C for two days. A dark green solid precipitated. The precipitate was filtered off, washed twice with 20 mL of hot DMF and dried in air. Yield: 78%. **Cu-BTPP** is insoluble in alcohols, chlorinated solvents, acetonitrile, DMSO, DMF, acetone and H_2O. Elem. Anal. calc. for $C_{42}H_{45}Cu_3N_9O_5$ (FW = 946.46 g mol^{-1}): C, 53.29; H, 4.79; N, 13.31%. Found: C, 53.21; H, 4.66; N, 12.94%. IR (neat, cm^{-1}): 3400(br), 3030(vw) ν(C–$H_{aromatic}$), 2929(w) ν(C–$H_{aliphatic}$), 1670(vs) ν(C═O), 1560(s), 1501(w) ν(C═C + C═N), 1384(s), 1255(s), 1176(m), 1091(s), 1053(s), 954(s), 822(vs), 660(m).

A special comment is required for understanding the correct formulation of **Cu-BTPP**. Since X-rays, and particularly X-ray powder diffraction methods, are blind to the presence of H atoms, the nature of the central O atom, which could correspond to either a hydroxo or an oxo ligand, comes into question. However, if we were in the presence of a O^{2-} moiety capping the Cu_3 triangle, the conundrum of a mixed-valence compound would not disappear, as a $Cu^ICu_2^{II}(O)(BTPP)$ formulation would be still necessary. The experimentally measured magnetic moment (2.34μ_B per trinuclear unit at 295 K) is not diagnostic, as it may be explained by either a cooperative behavior of the Cu(II) ions mediated by the ligands, or the dilution of the Cu(II) centers by the diamagnetic Cu(I) ones. In addition, infrared spectroscopy, in the presence of water molecules and aerial moisture into the cavities, cannot be taken as a definitive probe. With the complementary observations that the majority of $Cu_3N_6(\mu_3\text{-}O)$ fragments found in the Cambridge Structural Database bear an oxygen-bound H-atom, and that, under the relatively mild (and *far from being basic*) synthetic conditions described above, the formation of O^{2-} anions should not be favored, the proposed formulation, with a hydroxo anion and single Cu(II) center, in our opinion, should be chosen.

X-ray powder diffraction structural analysis

Polycrystalline samples of **Ni-BTPP** and **Cu-BTPP**, not containing single crystals, were ground in an agate mortar. Then, they were deposited in the hollow of an aluminum-framed sample holder equipped with a quartz zero-background plate. For both compounds, preliminary data acquisitions were carried out at room temperature in the 2θ range of 3–35°, with steps of 0.02°, on a Bruker AXS D8 Advance diffractometer, equipped with Ni-filtered Cu Kα radiation (λ = 1.5418 Å), a Lynxeye linear position-sensitive detector, and the following optics: primary beam Soller slits (2.3°), fixed divergence slit (0.5°), receiving slit (8 mm). These preliminary acquisitions revealed the rather low crystallinity of the two materials, less than ten broad peaks emerging from the structured background (Fig. S1 of the ESI†). To carry out the structure determinations, another set of diffraction data was collected by means of overnight scans in the 2θ range of 3-105°, with steps of 0.02°. In spite of the low crystallinity degree, peak search, followed by indexing through the singular value decomposition approach[15] implemented in TOPAS-R,[16] allowed the detection of the approximate unit cell parameters of both the species. The space group of **Cu-BTPP** was assigned coupling the presence of systematic absences to geometrical considerations upon the special positions that could be occupied by both the ligand and the metal ion. More in detail, the PXRD pattern of **Cu-BTPP** does not contain peaks retraceable to *hkl* triplets with $l \neq$ zero. Hence, the crystallographic axis ***c*** is in principle undetermined. Indeed, by imposing the value of ***c*** as low enough as to avoid the presence of *hkl* reflections with $l \neq 0$ within the Cu Kα sphere, the diffraction pattern can be successfully modeled (Fig. S2†) by a *2-D structural model*, *i.e.* a crystal structure projected onto the *ab* plane, an approach already reported in ref. 17. An approximate value can be attributed to ***c*** as a multiple of 3.2 Å (namely 6.4 Å), due to the presence of a broad halo centered at 2θ = 28.1°. This attribution allowed us to propose an ideal structure in $P6_3/mmc$. Nonetheless, the crystalline coherent domains possess an average dimension of 37 nm in the *ab* plane, and of only a few nm along **c**. This occurrence indicates a clearly limited growth along **c**, the direction along which the 2-D layers pack. Prior to the structure solution, the unit cell and space group of **Cu-BTPP** were verified by means of a Le Bail refinement. The structure solution was performed by the simulated annealing technique, implemented in TOPAS-R, employing an idealized model for the crystallographic independent portion of the ligand.[18] Due to the highly structured background, the localization of (possibly disordered) solvent molecules was unfeasible. Thus, at the final stages of the structure solution, the electronic density of the solvent was modeled by means of dummy atoms located into the one-dimensional channels, with refined site occupation factors.

In spite of the numerous attempts, the cubic I[19] crystal structure of **Ni-BTPP** remains presently unsolved. The final refinement of the crystal structure of **Cu-BTPP** was carried out by the Rietveld method,[20] maintaining the rigid body introduced at the solution stage. The peak shapes were described with the fundamental parameters approach.[21] The background was modeled by a Chebyshev polynomial. One, isotropic thermal parameter was assigned to the metal atoms (B_M) and refined; lighter atoms were given a $B_{iso} = B_M + 2.0$ Å^2 thermal parameter. The peak shape anisotropy was modeled with the aid of spherical harmonics.

Fractional atomic coordinates are supplied in the ESI† as a CIF file. X-ray crystallographic data in CIF format have been deposited at the Cambridge Crystallographic Data Center as supplementary publication no. 1054571.

Crystallographic data for $Cu^{I}_2Cu^{II}(OH)(BTPP)\cdot 3DMF\cdot H_2O$, **Cu-BTPP**: hexagonal, $P6_3/mmc$, Z = 2, a = 20.925(9) Å, c = 6.4 Å, V = 2427(2) Å^3; $F(000)$ = 974; ρ = 1.27 g cm^{-3}; μ = 18.77 cm^{-1}; R_p = 0.036, R_{wp} = 0.048, R_{Bragg} = 0.63 for 5051 observations and 25 parameters. Please note that the unreasonably low value of the R_{Bragg} figure of merit is due to the highly structured background characterizing the powder diffraction pattern of **Cu-BTPP**.

Gas adsorption measurements

Gas adsorption isotherms were measured by the volumetric method using an ASAP2020 analyzer (Micrometrics Instruments Corp., Norcross, GA). Measurements of N_2 adsorption were carried out at 77 K for relative pressures in the range of 0–1 bar; CO_2 adsorption measurements were performed at 298 K for absolute pressures in the range of 0–1.2 bar. A sample of ~150 mg of as-synthesized compound was introduced into a pre-weighed analysis tube (1.3 cm diameter, 10 cm^3 bulb), which was capped with a gas-tight Transeal to prevent intrusion of oxygen and atmosphere moisture during transfer and weighing. The sample was evacuated under dynamic vacuum at 250 °C (**Ni-BTPP**) or 200 °C (**Cu-BTPP**), until an outgas rate of less than 2 mTorr per min (0.27 Pa min^{-1}) was achieved. The analysis tube containing the desolvated sample was then weighed again, to determine the mass of the sample, and transferred back to the analysis port of the gas sorption instrument. The outgas rate was confirmed to be less than 2 mTorr per min. For all of the isotherms, warm and cold free space correction measurements were performed using ultra high purity He gas (UHP-grade 5.0, 99.999% purity). N_2 isotherms at 77 K were measured in a liquid nitrogen bath using UHP-grade gas sources.

Results and discussion

Synthesis of H_3BTPP

The overall synthesis of the ligand is represented in Scheme S1,† provided in the ESI.† Briefly, by the Suzuki coupling reaction of 1,3,5-tris(4-bromophenyl)benzene and 1-(tetrahydro-pyran-2-yl)-4-pyrazoleboronic acid pinacol ester in a mixture of dioxane and water (1 : 1 by volume) and in the presence of anhydrous potassium carbonate, tetrakis(triphenylphosphine)palladium and lithium chloride, the protected ligand 1,3,5-tris(((1-(tetrahydro-pyran-2-yl)-

pyrazol-4-yl)phenyl)benzene was isolated in good yield and purified by column chromatography. The subsequent deprotection in ethanol with 1 M HCl, under reflux, promoted the formation of H_3BTPP. The latter was purified by suspending it into a boiling mixture of dimethylformamide and methanol (1 : 1 by volume), affording a white and air-stable powder soluble in methanol, dimethylformamide and dimethylsulfoxide. Elemental analysis, infrared spectroscopy, ^{1}H NMR and positive ESI mass spectrometry confirmed the synthesis of the desired compound. As suggested by infrared spectroscopy (Fig. S3 of the ESI†), adjacent H_3BTPP molecules interact in the solid by means of NH···N hydrogen bonds.[22] In Scheme 2, a summative sketch of the ligand's synthesis and subsequent preparation of the metal-organic frameworks **Cu-BTPP** and **Ni-BTPP** is given.

Synthesis of Ni-BTPP and Cu-BTPP

In order to discover the best route for obtaining the two MOFs, several screening reactions were conducted by varying conditions such as solvents, temperature, time, and concentrations. Powder X-ray diffraction and infrared spectroscopy were routinely applied in order to monitor the success of each reaction.

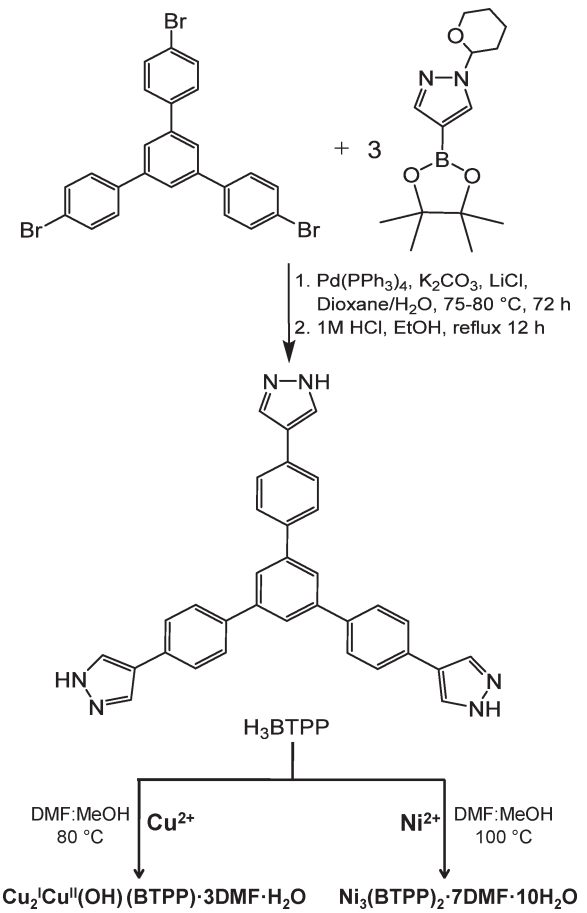

Scheme 2 Synthesis of H_3BTPP ligand and subsequent preparation of the two MOFs **Cu-BTPP** and **Ni-BTPP**.

Accordingly, **Ni-BTPP** was obtained by reacting H_3BTPP with nickel(II) perchlorate in 1 : 6 molar ratio in a 2 : 1 (v/v) mixture of DMF and methanol (Scheme 2). After heating at 100 °C for two days, an orange solid precipitated.

The composition of the product, $Ni_3(BTPP)_2{\cdot}7DMF{\cdot}10H_2O$, was corroborated by elemental analysis, thermogravimetric analysis, and infrared spectroscopy. Its formula reminds the expansion of the sodalite-type compound $Ni_3(BTP)_2$,[10d] but the diffraction patterns indicate that the two structures are not isostructural nor isomorphous.

Cu-BTPP was synthesized by heating H_3BTPP and copper(II) nitrate in 1 : 6 molar ratio at 80 °C for two days in a mixture of DMF and methanol (1 : 1 v/v) (Scheme 2). During the preliminary screening, it was observed that if heating is applied at or above 100 °C, a complete reduction of Cu(II) to Cu(I), accompanied by the formation of a reddish species (probably metallic copper or cuprous oxide), takes place. To avoid this undesired reduction, a reaction temperature of 80 °C was used and a dark green solid was isolated. Its chemical formula, as elucidated by elemental analysis, thermogravimetric analysis and infrared spectroscopy, is $Cu^{I}_2Cu^{II}(OH)(BTPP){\cdot}3DMF{\cdot}H_2O$, with copper ions in both +1 and +2 oxidation states. Thus, even at 80 °C, a partial reduction from Cu(II) to Cu(I) occurred to produce **Cu-BTPP** in the form of a mixed valence-based material. This occurrence was further confirmed by the structure determination (see the pertinent section). Notably, Ehlert *et al.* have previously described the heat-promoted formation of the mixed valence complex $Cu^{I}Cu^{II}_2(F_6dmpz)_5$ (F_6dmpz = 3,5-bis-(trifluoromethyl)-pyrazolate).[23]

Both **Ni-BTPP** and **Cu-BTPP** precipitate in high yields as air-stable powders that are insoluble in water and in most common solvents. Their infrared spectra (Fig. S4 and S5 of the ESI†) present quite similar absorption bands. In particular, the absence of N–H stretching bands indicates complete deprotonation of the organic linker along with the formation of metal-bridging tris(pyrazolate)-based trianions, as eventually confirmed by the structural analysis in the case of **Cu-BTPP**. As indicated by their infrared spectra, in both MOFs water and DMF molecules are present within the pores: the broad bands observed around 3400 cm^{-1} are due to the O–H stretching of water, while the very strong bands in the range 1640–1670 cm^{-1} can be assigned to the stretching of the carbonyl moiety of DMF.

Crystal structure analysis

The crystal structure of **Cu-BTPP** discussed here was determined by state-of-the-art powder diffraction methods applied to laboratory data. Relevant crystallographic details are collected in section 2.5.

Cu-BTPP crystallizes in the hexagonal space group $P6_3/mmc$. Its crystal structure is composed of triangular $[Cu_3N_6(OH)]$ nodes (Fig. 1a) lying perpendicular to the 6-fold crystallographic axes. The edges of each Cu_3 triangle are bridged by the pyrazolato moieties of three distinct $BTPP^{3-}$ ligands,

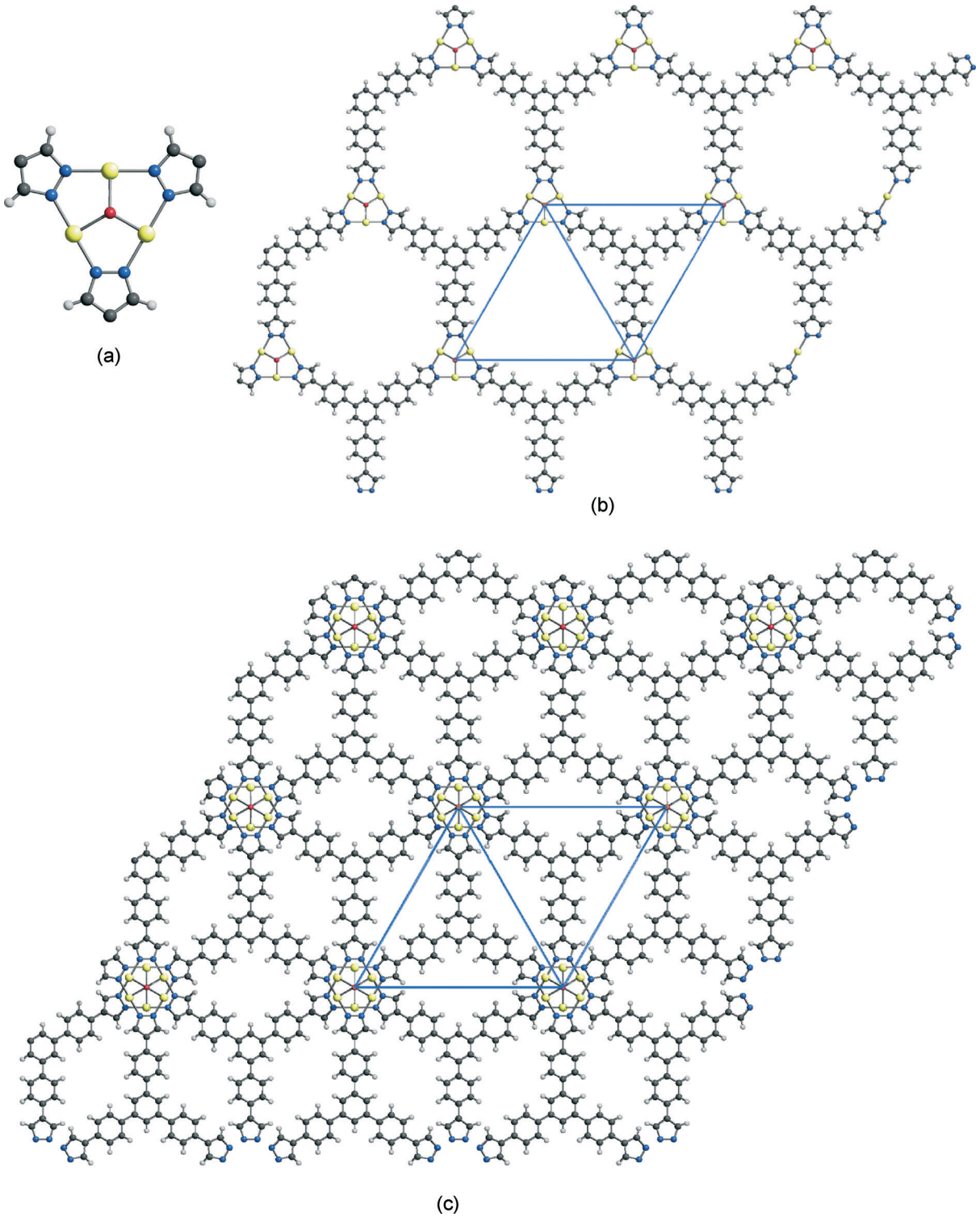

Fig. 1 Representation of the crystal structure of **Cu-BTPP**: a) the $[Cu_3N_6(OH)]$ node; b) one of the two-dimensional layers, viewed along the crystallographic axis ***c***; c) packing of the two-dimensional layers, viewed along the crystallographic axis ***c***. The one-dimensional slit-like channels can be appreciated from this view.

while a μ_3-OH group is located at its center, lying slightly above the plane formed by the copper and nitrogen atoms. Along the *ab* plane, each trimetallic node is connected to six nearby ones by the $BTPP^{3-}$ linkers, thus generating flat two-dimensional layers (Fig. 1b) stacking along the crystallographic axis *c* with a spacing equal to *c*/2 (Fig. 1c). This occurrence generates slit-like one-dimensional channels running along *c*, having an aperture of ~0.5 nm[24] and accounting for

a non-negligible amount of empty volume (51.5% of the unit cell volume[25]).

Incidentally, even if not very common, the $[Cu_3N_6(OH)]$ secondary building unit (SBU) is not unknown. Searching the 2014 version of the Cambridge Structural Database, it is possible to encounter this SBU in both monomeric[26] and dimeric[27] complexes, as well as in one-,[28] two-,[29] and three-dimensional[30] MOFs.

The isolation of a two-dimensional MOF should not be considered a failure with respect to the functional properties we aim to characterize. As a matter of fact, even if examples exist of low-dimensional frameworks that collapse when desolvated,[31] the presence of layers rather than a three-dimensional network does not necessarily prevent gas adsorption.[32] Notably, a number of two-dimensional frameworks have even shown structural flexibility,[32b,33] in that the relative positions of neighboring layers change as a result of external stimuli. Due to this, two-dimensional MOFs often show selective adsorption or gate-opening adsorption phenomena based on the expansion of the layers.[33a]

Thermal stability and activation

Thermogravimetric analyses (TGA) were performed on **Ni-BTPP** and **Cu-BTPP** in order to assess their thermal robustness along with their permanent porosity upon solvent removal by heating. The acquired TG traces of as-synthesized and evacuated samples are collected in Fig. 2 and 3, for **Ni-BTPP** and **Cu-BTPP**, respectively. Overall, both MOFs possess a remarkable thermal stability, decomposing at temperatures above 350 °C, thus confirming the key role of poly(pyrazolato)-based spacers in establishing strong metal-to-ligand coordinative bonds.

Upon heating, **Ni-BTPP** undergoes three consecutive weight losses in the temperature range 30–320 °C, amounting to approximately 36 wt%. The observed loss corresponds well

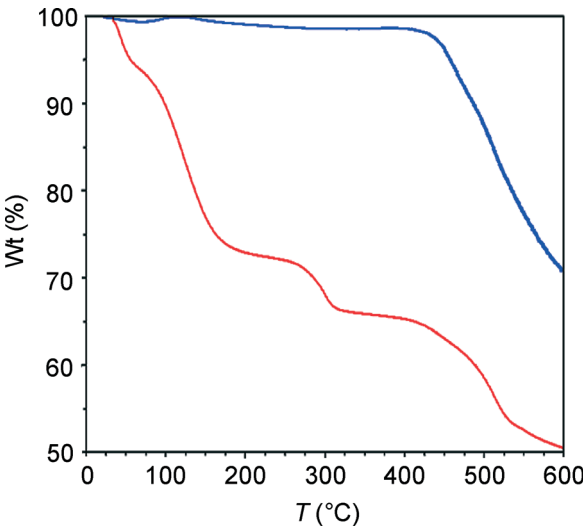

Fig. 2 Thermogravimetric analysis traces of **Ni-BTPP** as-synthesized (red) and after evacuation at 250 °C (blue).

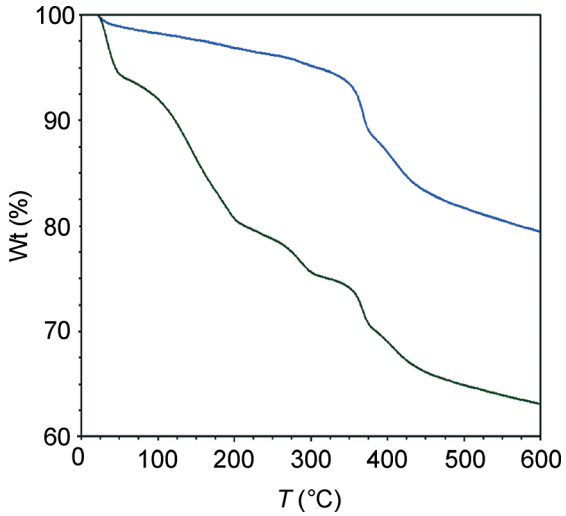

Fig. 3 Thermogravimetric analysis traces of **Cu-BTPP** as-synthesized (black) and after evacuation at 200 °C (blue).

to the expected value of 37 wt% for pore encapsulated water and DMF molecules. The evacuated material is stable until the onset of decomposition, at 450 °C. This observation indicates the remarkable robustness of the framework, as already featured by other nickel(II)-pyrazolate MOFs, such as Ni(BPEB) (H_2BPEB = 1,4-bis(1*H*-pyrazol-4-ylethynyl)benzene)[10a] and $Ni_3(BTP)_2$.[10d]

Prior to volumetric gas adsorption measurements, a sample of activated **Ni-BTPP** was analyzed to assess whether the removal of the guest molecules was complete after overnight evacuation at 250 °C under vacuum. The thermogravimetric analysis (Fig. 2) and elemental analysis[34] of the thermally treated batch confirmed the material was fully desolvated, while infrared spectroscopy (Fig. S5†) substantiated the structural integrity.

As-synthesized **Cu-BTPP** undergoes three consecutive solvent losses in the temperature range 30–325 °C, accounting for a total weight loss of approximately 26 wt%, corresponding to the removal of all water and DMF molecules trapped inside the porous framework (theoretical solvent amount 25 wt%). Evacuated **Cu-BTPP** is thermally stable up to the onset of its decomposition at 350 °C.

In preparation for gas adsorption measurements, a batch of **Cu-BTPP** was activated by heating overnight at 200 °C under dynamic vacuum. The sample was then analyzed to assess whether desolvation was complete and to check the structural integrity of the framework. The thermogravimetric analysis trace of the activated sample (Fig. 3) reveals a 2.5% weight loss in the temperature range 30–150 °C. This small weight loss is likely attributable to the adsorption of moisture from the air.[35] Infrared spectroscopy (Fig. S5†) confirmed the structural integrity of **Cu-BTPP** following desolvation.

Finally, as preliminary test to verify the water stability of the two title MOFs, powdered samples of both were suspended for 48 h in water at room temperature. The PXRD

patterns of recovered samples demonstrated that neither phase change, nor loss of crystallinity occurred.

Gas adsorption properties

The porosities of thermally activated compounds **Ni-BTPP** and **Cu-BTPP** were probed by N_2 adsorption measurements at 77 K. Moreover, CO_2 adsorption was probed at 298 K in the range of absolute pressures 0–1.2 bar. Key parameters obtained from the N_2 adsorption isotherms are listed in Table 1.

Both materials exhibit a type I adsorption isotherm (Fig. 4), with a sharp knee at low relative pressures (p/p_0 ~ 0.01), corresponding to primary micropore filling, followed by a plateau, suggesting that the porosity of the two MOFs is mainly due to the presence of micropores of uniform size. The presence of an H4-type hysteresis loop[36] in the isotherm of **Cu-BTPP** may be reasonably related to the presence of slit-like pores in its crystal structure.[37] Fitting the two N_2 isotherms afforded estimated BET surface areas of 1636(11) and 660(4) $m^2\ g^{-1}$ and Langmuir surface areas of 1923(3) and 874(8) $m^2\ g^{-1}$ for **Ni-BTPP** and **Cu-BTPP**, respectively.

Utilizing CO_2 at 298 K as the adsorptive, **Ni-BTPP** was found to adsorb 1.73 mmol g^{-1} (7.6 wt%) at 1 bar (Fig. 5). On the contrary, CO_2 was not adsorbed by **Cu-BTPP** under the same conditions. The CO_2 adsorption isotherm of **Ni-BTPP** is nearly linear, suggesting that the adsorption sites on this material are quite weak and relatively homogenous. By applying the Henry's law[38]

$$c = K_p p$$

where c = guest concentration (in mol kg^{-1}), and p = pressure (in bar), a Henry's Law constant K_p of 1.82 mol kg^{-1} bar^{-1} was calculated, further indicating limited CO_2 adsorption.

To the best of our knowledge, less than ten nickel(II)-based three-dimensional MOFs have been tested up to now as adsorbents of CO_2 at 298 K and 1 bar. The amount of CO_2 adsorbed by **Ni-BTPP** is between the extreme values of 0.9 wt%, shown by Ni(DBM)$_2$(bpy)[39] (DBM$^-$ = dibenzoylmethanate, bpy = 4,4′-bipyridine), and 23 wt%, obtained with Ni_2(dobdc) (dobdc^{4-} = 2,5-dioxidobenzene-1,4-dicarboxylate), and is comparable to the moderate values of 9.2 and 8.9 wt% attained with SNU-M10[40] (H_4bptc = 1,1′-biphenyl-3,3′,5,5′-tetracarboxylic acid) and Ni_3(*L*-TMTA)$_2$(bpy)$_4$[41] (*L*-H_3TMTA = trimesoyltri(*L*-alanine)), respectively.

The quantity of gas adsorbed at 1 bar is principally dependent on the specific surface area of the material. To observe

Table 1 Key parameters retrieved from the N_2 adsorption isotherms of **Ni-BTPP** and **Cu-BTPP**

Compound	BET SSA ($m^2\ g^{-1}$)	Langmuir SSA ($m^2\ g^{-1}$)	Adsorbed N_2 ($cm^3\ g^{-1}$ STP)
Ni-BTPP	1636(11)	1923(3)	441.7
Cu-BTPP	660(4)	874(8)	200.8

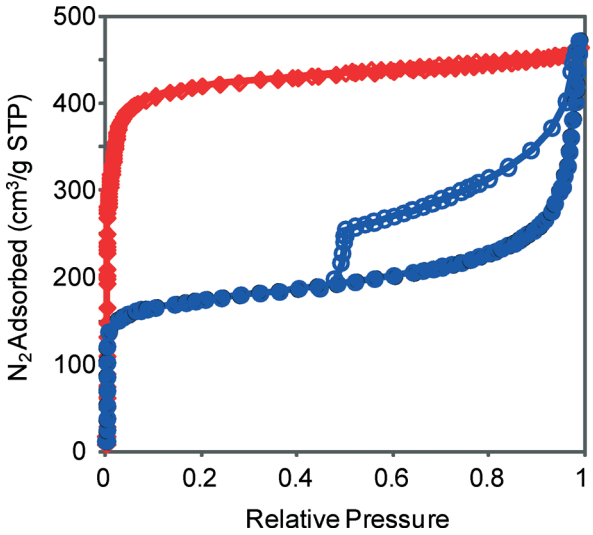

Fig. 4 Adsorption of N_2, as measured at 77 K for **Ni-BTPP** (red rhombi) and **Cu-BTPP** (blue circles). Filled and empty symbols denote the adsorption and desorption branches, respectively.

the role of the strongest adsorption sites, the initial slopes of the isotherms must be taken into consideration. At 0.1 bar, **Ni-BTPP** adsorbs only 1.0 wt%, which is roughly comparable to the value of 1.8 wt% shown by $Ni_3(BTP)_2$[42] and much less than the value of 11.0 wt% detected in the case of Ni_2(dobdc).[43] As far as $Ni_3(BTP)_2$ is concerned, a theoretical investigation[42] demonstrated the absence of a positive region around the square planar Ni(II) ions on the electrostatic potential, this allowing the authors to explain the scarce affinity of the four-coordinate metal centers toward CO and CO_2, as indicated by infrared spectroscopy. At variance, based on infrared spectroscopy and powder X-ray diffraction, it was shown that the square pyramidal stereochemistry of the Ni(II) ions in Ni_2(dobdc) is completed by one end-on CO_2 molecule.[43] Based on these evidences, to explain the very modest performances of **Ni-BTPP** at 0.1 bar, we tentatively propose that, as in the parent phase $Ni_3(BTP)_2$, the nickel(II) centers are surrounded by a positive electrostatic potential, such that no strong interaction is developed between the metal centers and the gas probe. Investigating the solid state Vis absorption of **Ni(BTPP)** did not provide a definitive proof on the coordination geometry of its metal centers. Indeed, by suspending **Ni(BTPP)** powders in ethanol, we observed a very weak and featureless absorption band (centered at 512 nm). This occurrence has been already pointed out in a number of papers. Significantly, in ref. 44 calculated DOS was presented and discussed for Ni(BPZ) and Ni(BDP) (H_2BPZ = 4,4′-bispyrazole; H_2BDP = 1,4-bis(4-pyrazolyl)benzene), showing that materials of this class behave as low-band gap semiconductors, with a broad and steep reflectance curve, which was interpreted as originating from ligand-to-metal charge transfer transitions (LMCTs). In line with this, the band detected for **Ni(BTPP)** at *ca.* 510 nm can be ascribed to LMTCs, hiding the weaker d–d electronic transitions which, for square planar Ni(II) ions, are observed in the same spectral region.

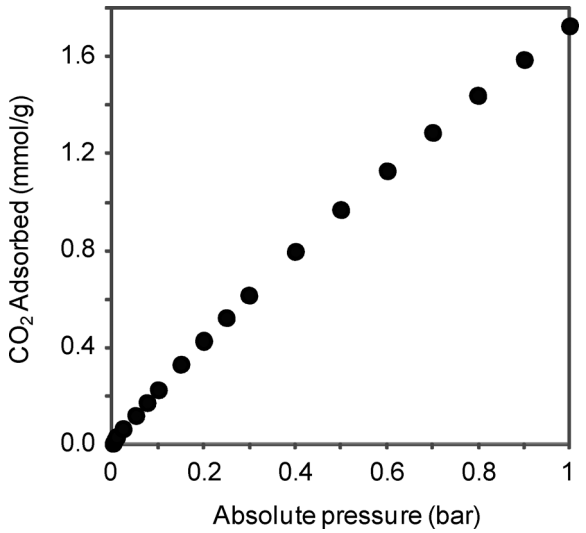

Fig. 5 Excess CO_2 adsorption isotherm measured at 298 K for **Ni-BTPP**.

Needless to say, the low degree of crystallinity of **Ni(BTPP)**, denouncing a limited three-dimensional periodicity of the network, hence of the pores, cannot be *a priori* discarded as a co-factor concurring to limit the adsorption performances of this material in the pressure range explored.

Conclusions

Two new metal-organic frameworks, namely $Ni_3(BTPP)_2$ (**Ni-BTPP**) and $Cu^{I}_4Cu^{II}_2(OH)_2(BTPP)_2$ (**Cu-BTPP**), were synthesized from the tritopic pyrazolate-based ligand 1,3,5-tris((1*H*-pyrazol-4-yl)phenyl)benzene (H_3BTPP). The crystal structure of **Cu-BTPP** bears triangular $[Cu_3N_6(\mu_3\text{-}OH)]$ nodes connected to six nearby ones by the linkers, thus constructing flat two-dimensional layers defining slit-like channels. Both MOFs are thermally robust, with **Ni-BTPP** decomposing only at the remarkably high temperature of 450 °C. As demonstrated by N_2 adsorption at 77 K, both materials possess permanent porosity, with Langmuir specific surface areas of 1923(3) and 874(8) $m^2\ g^{-1}$ for **Ni-BTPP** and **Cu-BTPP**, respectively. Finally, **Ni-BTPP** adsorbs 1.73 mmol g^{-1} (7.6 wt%) of CO_2 at the 298 K and 1 bar.

Acknowledgements

This work was supported by PRIN-2010–BNZ3F2 project DESCARTES of the Italian Ministry of the University and Research and by PRAT 2009 "Design, synthesis and characterization of coordination polymers by assembling of oligonuclear metal systems and polytopic ligands". The synthesis of these compounds and their characterization by spectroscopic, thermogravimetric, and gas adsorption measurements was funded by the Center for Gas Separations Relevant to Clean Energy Technologies, an Energy Frontier Research Center funded by the Department of Energy, Office of Science, Office of Basic Energy Sciences under award DE-SC0001015. Dr. Brian Weirs and Dr. Eric Bloch are gratefully acknowledged for helpful experimental assistance, and the Universities of Camerino and Insubria are thanked for additional funding. The courtesy of Professor Fabio Ferri, Università dell'Insubria, in acquiring the solid state Vis absorption spectrum of **Ni(BTPP)** is acknowledged.

Notes and references

1 See *e.g.* (*a*) *Metal-Organic Framework Materials*, ed. L. R. MacGillivray and C. M. Lukehart, John Wiley & Sons, 2014; (*b*) the themed issue by *Chem. Soc. Rev.*, ed. S. Kitagawa and H.-C. Zhou 2014, vol. 43, pp. 5415–6172; (*c*) the themed issue by *Chem. Rev.*, ed. H.-C. Zhou, J. R. Long and O. M. Yaghi, 2012, vol. 112, pp. 673–1268; (*d*) S. R. Batten, S. M. Neville and D. R. Turner, *Coordination Polymers: Design, Analysis and Application*, Springer, New York, 2010.

2 For luminescent MOFs see *e.g.* (*a*) J. Heine and K. Müller-Buschbaum, *Chem. Soc. Rev.*, 2013, **42**, 9232; (*b*) M. D. Allendorf, C. A. Bauer, R. K. Bhakta and R. J. T. Houk, *Chem. Soc. Rev.*, 2009, **38**, 1330.

3 See *e.g.* D.-F. Weng, Z.-M. Wang and S. Gao, *Chem. Soc. Rev.*, 2011, **40**, 3157.

4 For the use of MOFs in adsorption see *e.g.* (*a*) J. Canivet, A. Fateeva, Y. Guo, B. Coasne and D. Farrusseng, *Chem. Soc. Rev.*, 2014, **43**, 5594; (*b*) Y. He, W. Zhou, G. Qian and B. Chen, *Chem. Soc. Rev.*, 2014, **43**, 5657; (*c*) M. P. Suh, H. J. Park, T. K. Prasad and D.-W. Lim, *Chem. Rev.*, 2012, **112**, 782; (*d*) K. Sumida, D. L. Rogow, J. A. Mason, T. M. McDonald, E. D. Bloch, Z. R. Herm, T.-H. Bae and J. R. Long, *Chem. Rev.*, 2012, **112**, 724; (*e*) H. Wu, Q. Gong, D. H. Olson and J. Li, *Chem. Rev.*, 2012, **112**, 836.

5 For the use of MOFs as catalysts see *e.g.* (*a*) J. Liu, L. Chen, H. Cui, L. Zhang, J. Zhang and C.-Y. Su, *Chem. Soc. Rev.*, 2014, **43**, 6011; (*b*) M. Yoon, R. Srirambalaji and K. Kim, *Chem. Rev.*, 2012, **112**, 1196; (*c*) A. Corma, H. Garcia and F. X. Llabrés i Xamena, *Chem. Rev.*, 2010, **110**, 4606.

6 For the use of MOFs in separation see *e.g.* (*a*) B. Van de Voorde, B. Bueken, J. Denayer and D. De Vos, *Chem. Soc. Rev.*, 2014, **43**, 5766; (*b*) S. Qiu, M. Xue and G. Zhu, *Chem. Soc. Rev.*, 2014, **43**, 6116; (*c*) J.-R. Li, J. Sculley and H.-C. Zhou, *Chem. Rev.*, 2012, **112**, 869.

7 For the use of MOFs in drug delivery and imaging see *e.g.* (*a*) P. Horcajada, R. Gref, T. Baati, P. K. Allan, G. Maurin, P. Couvreur, G. Férey, R. E. Morris and C. Serre, *Chem. Rev.*, 2012, **112**, 1232; (*b*) J. Della Rocca, D. Liu and W. Lin, *Acc. Chem. Res.*, 2011, **44**, 957.

8 M. Zhang, M. Bosch, T. Gentle and H. Zhou, *CrystEngComm*, 2014, **16**, 4069.

9 J.-P. Zhang, Y.-B. Zhang, J.-B. Lin and X.-M. Chen, *Chem. Rev.*, 2012, **112**, 1001.

10 See *e.g.* (*a*) S. Galli, A. Maspero, C. Giacobbe, G. Palmisano, L. Nardo, A. Comotti, I. Bassanetti, P. Sozzani and N. Masciocchi, *J. Mater. Chem. A*, 2014, **2**, 12208; (*b*) Z. R. Herm, B. M. Wiers, J. A. Mason, J. M. van Baten, M. R. Hudson, P. Zajdel, C. M. Brown, N. Masciocchi, R. Krishna

and J. R. Long, *Science*, 2013, **340**, 960; (*c*) C. Pettinari, A. Tabacaru, I. Boldog, K. V. Domasevitch, S. Galli and N. Masciocchi, *Inorg. Chem.*, 2012, **51**, 5235; (*d*) V. Colombo, S. Galli, H. J. Choi, G. D. Han, A. Maspero, G. Palmisano, N. Masciocchi and J. R. Long, *Chem. Sci.*, 2011, **2**, 1311; (*e*) H. J. Choi, M. Dincă, A. Dailly and J. R. Long, *Energy Environ. Sci.*, 2010, **3**, 117; (*f*) J.-P. Zhang and S. Kitagawa, *J. Am. Chem. Soc.*, 2008, **130**, 907.

11 See *e.g.* (*a*) P. Yang, M.-X. Li, M. Shao, M.-S. Wang, S.-X. Cao, J.-C. Zhang and H.-H. Zhang, *Cryst. Growth Des.*, 2013, **13**, 4305; (*b*) G. A. Senchyk, A. B. Lysenko, E. B. Rusanov, A. N. Chernega, J. Jezierska, K. V. Domasevitch and A. Ozarowski, *Eur. J. Inorg. Chem.*, 2012, **35**, 5802; (*c*) K. Liu, W. Shi and P. Cheng, *Dalton Trans.*, 2011, **40**, 8475; (*d*) E. V. Govor, A. B. Lysenko, E. B. Rusanov, A. N. Chernega, H. Krautscheid and K. V. Domasevitch, *Z. Anorg. Allg. Chem.*, 2010, **636**, 209; (*e*) A. Demessence, D. M. D'Alessandro, M. L. Foo and J. R. Long, *J. Am. Chem. Soc.*, 2009, **131**, 8784.

12 See *e.g.* (*a*) I. Boldog, K. V. Domasevitch, J. K. Maclaren, C. Heering, G. Makhloufi and C. Janiak, *CrystEngComm*, 2014, **16**, 148; (*b*) I. Timokhin, J. B. Torres, A. J. P. White, P. D. Lickiss, C. Pettinari and R. P. Davies, *Dalton Trans.*, 2013, **42**, 13806; (*c*) Q. Lin, T. Wu, S.-T. Zheng, X. Bu and P. Feng, *J. Am. Chem. Soc.*, 2012, **134**, 784; (*d*) M.-N. Li, G.-S. Yang, S.-L. Li, H.-Y. Zang, G.-J. Xu, K.-Z. Shao and Z.-M. Su, *Inorg. Chem. Commun.*, 2010, **13**, 1203; (*e*) M. Dincă, A. Dailly, Y. Liu, C. M. Brown, D. A. Neumann and J. R. Long, *J. Am. Chem. Soc.*, 2006, **128**, 16876; (*f*) M. Dincă, A. Dailly, C. Tsay and J. R. Long, *Inorg. Chem.*, 2008, **47**, 11.

13 pK_a(tetrazole) 4.9; pK_a(1,2,3-triazole) = 13.9; pK_a(pyrazole) = 19.8. These values are taken from F. G. Bordwell, *Acc. Chem. Res.*, 1988, **21**, 456 and are referenced to DMSO.

14 J. Angbrant, E. Homan, T. Lundbaek, J. Martinsson, M. Sari, M. Joensson, K. Faernegaardh and K. Hallberg, WO2011161201, 2011, Kancera AB, Sweden.

15 A. Coelho, *J. Appl. Crystallogr.*, 2003, **36**, 86.

16 *TOPAS Version 3.0, Bruker AXS*, Karlsruhe, Germany, 2005.

17 X. Ribas, A. Sironi, N. Masciocchi, E. B. Lopes, M. Almeida, J. Veciana and C. Rovira, *Inorg. Chem.*, 2005, **44**, 2358.

18 To describe the crystallographically independent portion of the H_3BTPP ligand, the z-matrix formalism was used, imposing idealized bond distances and angles, as follows: C–C, C–N, N–N of the penta-atomic ring 1.36 Å; C–C of the hexa-atomic rings 1.39 Å; exocyclic C–C 1.50 Å; C–H, N–H 0.95 Å; penta-atomic ring internal bond angles 108°; penta-atomic ring external bond angles 126°; hexa-atomic rings internal and external bond angles 120°.

19 a = 23.139(1) Å, V = 12388(1) Å^3.

20 R. A. Young, *The Rietveld Method, IUCr Monograph N. 5*, Oxford University Press, New York, 1981.

21 R. W. Cheary and A. Coelho, *J. Appl. Crystallogr.*, 1992, **25**, 109.

22 K. Nakamoto, *Infrared and Raman Spectra of Inorganic and Coordination Compounds, Part B, Applications in Coordination, Organometallic, and Bioinorganic Chemistry*, 2009, 6th edn, Wiley.

23 M. K. Ehlert, A. Storr, D. A. Summers and R. C. Thompson, *Can. J. Chem.*, 1997, **75**, 491.

24 Calculated as the distance between two opposite hydrogen atoms along the channels, taken into account their van der Waals radius (1.20 Å).

25 A. L. Spek, *J. Appl. Crystallogr.*, 2003, **36**, 7–13Calculated with PLATON after solvent removal.

26 (*a*) X.-Y. Wu, X.-F. Kuang, Z.-G. Zhao, S.-C. Chen, Y.-M. Xie, R.-M. Yu and C.-Z. Lu, *Inorg. Chim. Acta*, 2010, **363**, 1236; (*b*) M. Bichay, J. W. Fronabarger, R. Gilardi, R. J. Butcher, W. B. Sanborn, M. E. Sitzmann and M. D. Williams, *Tetrahedron Lett.*, 2006, **47**, 6663; (*c*) X. Liu, M. P. de Miranda, E. J. L. McInnes, C. A. Kilner and M. A. Halcrow, *Dalton Trans.*, 2004, 59; (*d*) J.-C. Liu, G.-C. Guo, J.-S. Huang and X.-Z. You, *Inorg. Chem.*, 2003, **42**, 235; (*e*) A. V. Virovets, N. V. Podberezskaya and L. G. Lavrenova, *Zh. Strukt. Khim.*, 1997, **38**, 532.

27 K. Sakai, Y. Yamada, T. Tsubomura, M. Yabuki and M. Yamaguchi, *Inorg. Chem.*, 1996, **35**, 542.

28 See *e.g.* (*a*) E. V. Lider, E. V. Peresypkina, A. I. Smolentsev, V. N. Elokhina, T. I. Yaroshenko, A. V. Virovets, V. N. Ikorskii and L. G. Lavrenova, *Polyhedron*, 2007, **26**, 1612; (*b*) M. Casarin, C. Corvaja, C. Di Nicola, D. Falcomer, L. Franco, M. Monari, L. Pandolfo, C. Pettinari, F. Piccinelli and P. Tagliatesta, *Inorg. Chem.*, 2004, **43**, 5865.

29 See *e.g.*(*a*) C. Pettinari, N. Masciocchi, L. Pandolfo and D. Pucci, *Chem. – Eur. J.*, 2010, **16**, 1106; (*b*) M. Casarin, C. Corvaja, C. Di Nicola, D. Falcomer, L. Franco, M. Monari, L. Pandolfo, C. Pettinari and F. Piccinelli, *Inorg. Chem.*, 2005, **44**, 6265.

30 See *e.g.* (*a*) E.-C. Yang, Z.-Y. Liu, C.-H. Zhang, Y.-L. Yang and X.-J. Zhao, *Dalton Trans.*, 2013, **42**, 1581; (*b*) G. A. Senchyk, A. B. Lysenko, I. Boldog, E. B. Rusanov, A. N. Chernega, H. Krautscheid and K. V. Domasevitch, *Dalton Trans.*, 2012, **41**, 8675; (*c*) S. Ferrer, E. Anar, F. Lloret, A. Castineiras, M. Liu-Gonzalez and J. Borras, *Inorg. Chem.*, 2007, **46**, 372; (*d*) Y. Wang, P. Cheng, Y. Song, D.-Z. Liao and S.-P. Yan, *Chem. – Eur. J.*, 2007, **13**, 8131; (*e*) A. B. Lysenko, E. V. Govor, H. Krautscheid and K. V. Domasevitch, *Dalton Trans.*, 2006, 3772.

31 See *e.g.* (*a*) S. Kitagawa and K. Uemura, *Chem. Soc. Rev.*, 2005, **34**, 109; (*b*) S. Kitagawa, R. Kitaura and S. Noro, *Angew. Chem., Int. Ed.*, 2004, **43**, 2334.

32 See *e.g.* (*a*) A. Tabacaru, C. Pettinari, F. Marchetti, S. Galli and N. Masciocchi, *Cryst. Growth Des.*, 2014, **14**, 3142; (*b*) Y. Hijikata, S. Horike, M. Sugimoto, T. Fukushima and S. Kitagawa, *Inorg. Chem.*, 2013, **52**, 3634; (*c*) S.-I. Noro, Y. Hijikata, M. Inukai, T. Fukushima, S. Horike, M. Higuchi, S. Kitagawa, T. Akutagawa and T. Nakamura, *Inorg. Chem.*, 2013, **52**, 280; (*d*) B. Mu, F. Li and K. S. Walton, *Chem. Commun.*, 2009, 2493.

33 See *e.g.* (*a*) A. Kondo, H. Noguchi, S. Ohnishi, H. Kajiro, A. Tohdoh, Y. Hattori, W. C. Xu, H. Tanaka, H. Kanoh and K. Kaneko, *Nano Lett.*, 2006, **6**, 2581; (*b*) R. Kitaura, K. Seki, G. Akiyama and S. Kitagawa, *Angew. Chem., Int. Ed.*, 2003, **42**, 428.

34 Elem. Anal. Obs. for thermally activated **Ni-BTPP:** C, 59.03; H, 3.43; N, 12.68%. Calcd. for $Ni_3(BTPP)_2$: C, 58.49; H, 3.12; N, 12.40%.
35 Elem. Anal. Obs. for thermally activated **Cu-BTPP:** C, 55.02; H, 3.26; N, 11.39%. Calcd. for $Cu^{I}_2Cu^{II}(OH)(BTPP)\cdot H_2O$: C, 54.50; H, 3.32; N, 11.55%.
36 F. Rouquerol, J. Rouquerol and K. S. S. Singh, *Adsorption by powders and porous solids*, Academic Press, New York, 1999.
37 K. S. W. Sing, D. H. Everett, R. A. W. Haul, L. Moscou, R. A. Pierotti, J. Rouquérol and T. Siemieniewska, *Pure Appl. Chem.*, 1985, **57**, 603.
38 T. L. P. Dantas, S. M. Amorim, F. M. T. Luna, I. J. Silva Junior, D. Azevedo, A. E. Rodrigues and R. F. P. M. Moreira, *Sep. Sci. Technol.*, 2010, **45**, 73.
39 J. T. Culp, A. L. Goodman, D. Chirdon, S. G. Sankar and C. Matranga, *J. Phys. Chem. C*, 2010, **114**, 2184.
40 H.-S. Choi and M. P. Suh, *Angew. Chem., Int. Ed.*, 2009, **48**, 6865.
41 Z. Chen, X. Liu, C. Zhang, Z. Zhang and F. Liang, *Dalton Trans.*, 2011, **40**, 1911.
42 G. C. Shearer, V. Colombo, S. Chavan, E. Albanese, B. Civalleri, A. Maspero and S. Bordiga, *Dalton Trans.*, 2013, **42**, 6450.
43 P. D. C. Dietzel, R. E. Johnsen, H. Fjellvag, S. Bordiga, E. Groppo, S. Chavan and R. Blom, *Chem. Commun.*, 2008, 5125.
44 E. Albanese, B. Civalleri, M. Ferrabone, F. Bonino, S. Galli, A. Maspero and C. Pettinari, *J. Mater. Chem.*, 2012, **22**, 2259.